J|A|C|S ARTICLES

Published on Web 11/18/2009

Exceptional Ion-Exchange Selectivity in a Flexible Open Framework Lanthanum(III)tetrakisphosphonate

Monika Plabst,[†] Lynne B. McCusker,[‡] and Thomas Bein*,[†]

Department of Chemistry and Biochemistry and Center for NanoScience (CeNS), University of Munich (LMU), Butenandtstrausse 11, 81377 Munich, Germany, and Laboratory of Crystallography, ETH Zurich, 8093 Zurich, Switzerland

Received June 8, 2009; E-mail: bein@lmu.de

Abstract: The flexible, anionic, open-framework material $NaLa[(PO_3H)_2CH-C_6H_4-CH(PO_3H)_2]\cdot 4H_2O$ (**NaLa(H_4L)**) exhibits an exceptional selectivity for monovalent metal cations. This study elucidates the relationship between the ion-exchange behavior and the framework flexibility of this recently discovered material. The exchange of the Na^+ ions in **NaLa(H_4L)** with alkaline-earth, alkaline, and selected transition metal ions was studied. EDX and ICP-OES elemental analysis revealed that ion exchange was successful with monovalent ions, while higher-valent ions were rejected. An explanation for this charge selectivity could be found in the site-specific role of the guest cation. X-ray diffraction and thermogravimetric studies on the reversible hydration and dehydration behavior demonstrate that **NaLa(H_4L)** has a flexible framework. Contraction of the channels upon dehydration leads to a decrease in the cell volume of 15%. Rietveld refinement of the structure of the dehydrated form **NaLa(H_4L)$_{dehyd}$** revealed the key role played by the guest cation in the channel-shrinking mechanism. In the hydrated, expanded form, each Na^+ ion guest shares three phosphonate oxygens with a La^{3+} ion in a lanthanum phosphonate chain that defines part of the wall of a rhombic channel. The Na^+ ion completes its octahedral coordination sphere with two water molecules and a weaker bond to a fourth phosphonate oxygen. In the dehydrated, contracted form, the Na^+ ion loses the two water molecules and moves toward a second La^{3+} ion, which is located in an adjacent lanthanum phosphonate chain, to share two more phosphonate oxygens, and becomes 5-coordinate. This results in the formation of an −La−O−Na−O−La− chain and a concomitant shrinking of the channels. A comparison of the monovalent metal (M(I)) ion-exchanged compounds, **M(I)La(H_4L)**, reveals that both the ionic radius and the enthalpy of hydration of the guest cation affect the equilibrium between the expanded and the contracted forms, and that the framework adapts specifically to the size of the guest cation.

Introduction

In the early days of research in the field of metal organic frameworks (MOFs), it was believed that rigidity of the host network was a prerequisite for their successful performance as porous materials, because it was assumed that flexibility would lead to a collapse of the structure.[1] This perspective has changed fundamentally. The discovery of a series of flexible porous coordination frameworks demonstrated that some MOF materials can change their cell volumes significantly (some of them by up to 40%[2] or even 170%[3]) while preserving their basic structures.[4−12] Representative examples include flexible porous carboxylates formed by chains of metallic centers[2,13,14] or metal-center trimers[15,16] ($M = Cr^{3+}$, Al^{3+}, Fe^{3+}) that are connected by organic linkers to form three-dimensional coordination networks. It could be shown that these structures adapt their pore sizes to the type and number of guest species, while the connections between the inorganic nodes and organic linkers remain intact.[3,13] In this process, weak interactions such as hydrogen bonding between the guest molecules and the framework play a decisive role[17] and can lead to selectivity for specific guest species.[18,19]

[†] University of Munich.
[‡] ETH Zürich.

(1) Kitagawa, S.; Kondo, M. *Bull. Chem. Soc. Jpn.* **1998**, *71*, 1739–1753.
(2) Serre, C.; Millange, F.; Thouvenot, C.; Nogues, M.; Marsolier, G.; Louer, D.; Ferey, G. *J. Am. Chem. Soc.* **2002**, *124*, 13519–13526.
(3) Serre, C.; Mellot-Draznieks, C.; Surble, S.; Audebrand, N.; Filinchuk, Y.; Ferey, G. *Science* **2007**, *315*, 1828–1831.
(4) Fletcher, A. J.; Cussen, E. J.; Prior, T. J.; Rosseinsky, M. J.; Kepert, C. J.; Thomas, K. M. *J. Am. Chem. Soc.* **2001**, *123*, 10001–10011.
(5) Barthelet, K.; Marrot, J.; Riou, D.; Ferey, G. *Angew. Chem., Int. Ed.* **2002**, *41*, 281–284.
(6) Kitaura, R.; Seki, K.; Akiyama, G.; Kitagawa, S. *Angew. Chem., Int. Ed.* **2003**, *42*, 428–431.
(7) Kubota, Y; Takata, M; Matsuda, R; Kitaura, R; Kitagawa, S; Kobayashi, T. C. *Angew. Chem., Int. Ed.* **2006**, *45*, 4932–4936.
(8) Zhao, X.; Xiao, B.; Fletcher, A. J.; Thomas, K. M.; Bradshaw, D.; Rosseinsky, M. J. *Science* **2004**, *306*, 1012–1015.
(9) Takamizawa, S.; Saito, T.; Akatsuka, T.; Nakata, E. *Inorg. Chem.* **2005**, *44*, 1421–1424.
(10) Li, D.; Kaneko, K. *Chem. Phys. Lett.* **2001**, *335*, 50–56.
(11) Fletcher, A. J.; Thomas, K. M.; Rosseinsky, M. J. *J. Solid State Chem.* **2005**, *178*, 2491–2510.
(12) Uemura, K.; Matsuda, R.; Kitagawa, S. *J. Solid State Chem.* **2005**, *178*, 2420–2429.
(13) Millange, F.; Serre, C.; Ferey, G. *Chem. Commun.* **2002**, 822–823.
(14) Whitfield, T. R.; Wang, X.; Liu, L.; Jacobson, A. J. *Solid State Sci.* **2005**, *7*, 1096–1103.
(15) Serre, C; Millange, F.; Surblé, S.; Férey, G. *Angew. Chem., Int. Ed.* **2004**, *43*, 6285–6289.
(16) Mellot-Draznieks, C.; Serre, C.; Surble, S.; Audebrand, N.; Ferey, G. *J. Am. Chem. Soc.* **2005**, *127*, 16273–16278.

10.1021/ja904636y

The adaptation of a framework to accommodate a specific guest has also been observed to a lesser extent in inorganic ion-exchange materials. In layered mixed oxides[20,21] and M(IV) phosphates,[22] for example, the spacing between two layers changes with the intercalated ion. The rigid three-dimensional open frameworks of zeolites, however, tend to be less affected by ion exchange. They have well-defined channels and cages that permit only ions up to a certain size to enter. For example, the zeolite analcime[23,24] excludes Cs^+ ions, and zeolite A excludes large tetraalkylammonium ions from its sodalite cages.[25] Nevertheless, most zeolites can accommodate a considerable number of uni- and/or divalent cations in their larger cavities. In equilibrium experiments, where two different cations are present, a specific zeolite often shows a preference for certain types or sizes of ions.[26,27] The selectivity depends mainly on the size of the pore opening, the electrostatic interactions between the anionic framework and the cationic guest, and the concentration of the ions in solution. As selectivity becomes more specific, the ability of the framework to adapt can also play a significant role in zeolitic three-dimensional structures. It was shown quite recently that the Cs^+-exchange mechanism in a tunnel-type titanium silicate,[28] which selectively captures Cs^+ and Sr^{2+} from highly concentrated $NaNO_3$ solutions,[29] is mediated by conformational changes in the framework.[30−32] These results suggest that flexible metal organic frameworks might be predestined to be selective ion exchangers. However, as most MOFs have neutral frameworks, the incorporation of ionic guests in this type of material has only been investigated in a limited number of cases.[33−37]

To examine this issue more closely, we undertook a combined study of the ion-exchange properties and the framework flexibility of the recently discovered NaLa[$(PO_3H)_2$-CH−C_6H_4−CH$(PO_3H)_2$]·$4H_2O$, **NaLa(H4L)**, a lanthanum tetrakisphosphonate with a three-dimensional coordination network.[38] Its anionic framework is constructed from La^{3+} ions and $(PO_3H)_2$CH−C_6H_4−CH$(PO_3H)_2$ ($\mathbf{H_4L^{4-}}$), a ligand with two bisphosphonate groups connected via a rigid benzene linker. The La^{3+} ions are bridged by the phosphonate groups of the $\mathbf{H_4L^{4-}}$ ligand to form −La−O−P−O−La− chains, and these chains are linked via the organic spacer to form a three-dimensional anionic open framework. The framework features rhombic channels, which are defined by the chains located at the corner of each rhombus and are filled with Na^+ ions and water molecules as guests (Figure 1).

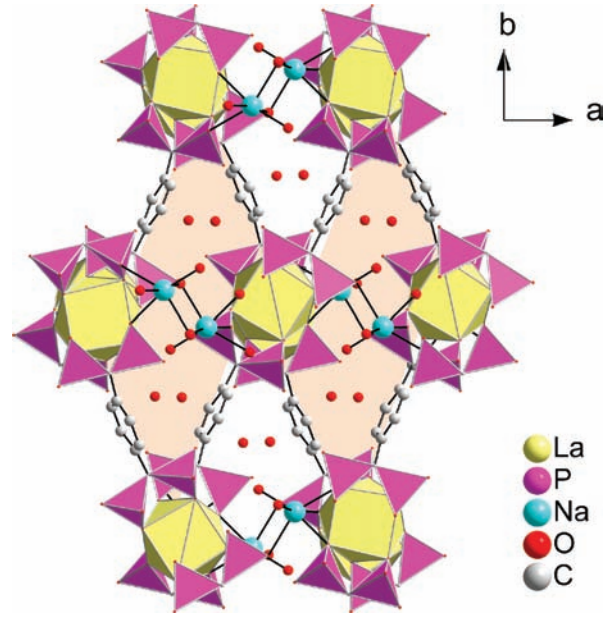

Figure 1. Projection of the **NaLa(H4L)** structure showing the rhombus (shaded) formed by the connection of phosphonate bridged chains of La^{3+} ions (perpendicular to the page) and the $\mathbf{H_4L^{4-}}$ ligand. The channels are filled with Na^+ ions and H_2O molecules.

Experimental Section

Metal salts were purchased from Aldrich in the purity degrees extra pure, p.a., puriss. or had a purity of more than 99.5%. NaOH was purchased as a 1 M volumetric standard solution. Bidistilled water from a Millipore system (Milli-Q Academic A10) was used throughout. The molecular building block 1,4-phenylenbis(methylidyne)tetrakis(phosphonic acid), $\mathbf{H_8L}$, was prepared as described elsewhere[38] and provided as a 0.5 M aqueous solution.

Synthesis of NaLa[$(PO_3H)_2$CH−C_6H_4−CH$(PO_3H)_2$]·$4H_2O$, NaLa(H4L). Water (7.94 mL (830 mmol)) and 4.00 mL of 1.0 M NaOH were added to 2.00 mL of a 0.5 M aqueous solution of $\mathbf{H_8L}$. Stirring was started, and 1 mL of 1 M $La(NO_3)_3$ was added. The gel with the batch composition $La(NO_3)_3$:H_8L:4 NaOH:830 H_2O was stirred for 30 min and then heated under hydrothermal conditions for 36 h at 100 °C. The precipitated crystals were separated from the reaction mixture by filtration under reduced pressure, washed with water, and dried at room temperature. The pH of the reaction mixture was 1.0 before and 1.5 after the heating process. (Yield: 630 mg, 0.96 mmol, 96%). Chemical analysis by EDX yielded La/Na/P = 1.1:1.3:4.0, and by ICP-OES La/Na/P = 1.0:1.1:4.0. Dehydration of **NaLa(H4L)** was effected by heating the as-synthesized form for 2 h at 180 °C in air. The dehydrated form NaLa[$(PO_3H)_2$CH−C_6H_4−CH$(PO_3H)_2$], $\mathbf{NaLa(H_4L)_{dehyd}}$, is stable if stored under vacuum, argon or nitrogen, but exposure to moist air results in rapid rehydration.

(17) Loiseau, T.; Serre, C.; Huguenard, C.; Fink, G.; Taulelle, F.; Henry, M.; Bataille, T.; Ferey, G. *Chem.−Eur. J.* **2004**, *10*, 1373–1382.
(18) Bourrelly, S.; Llewellyn, P. L.; Serre, C.; Millange, F.; Loiseau, T.; Ferey, G. *J. Am. Chem. Soc.* **2005**, *127*, 13519–13521.
(19) Llewellyn, P. L.; Bourrelly, S.; Serre, C.; Filinchuk, Y.; Ferey, G. *Angew. Chem., Int. Ed.* **2006**, *45*, 7751–7754.
(20) England, W. A.; Goodenough, J. B.; Wiseman, P. J. *J. Solid State Chem.* **1983**, *49*, 289–299.
(21) England, W. A.; Birkett, J. E.; Goodenough, J. B.; Wiseman, P. J. *Solid State Chem.* **1983**, *49*, 300–308.
(22) Clearfield, A. *Chem. Rev.* **1988**, *88*, 125–148.
(23) Barrer, R. M.; Sammon, D. C. *J. Chem. Soc.* **1956**, 675–682.
(24) Barrer, R. M.; Hinds, L. *J. Chem. Soc.* **1953**, 1879–1888.
(25) Barrer, R. M.; Meier, W. M. *Trans. Faraday Soc.* **1958**, *54*, 1074–1085.
(26) Sherry, H. S. In *Handbook of Zeolite Science and Technology*; Auerbach, S. M., Carrado, K. A., Dutta, P. K., Eds.; Marcel Dekker: New York, 2003; pp 1007−1062.
(27) Kuronen, M.; Harjula, R.; Jernstrom, J.; Vestenius, M.; Lehto, J. *Phys. Chem. Chem. Phys.* **2000**, *2*, 2655–2659.
(28) Clearfield, A. *Solid State Sci.* **2001**, *3*, 103–112.
(29) Zheng, Z.; Gu, D.; Anthony, R. G.; Klavetter, E. *Ind. Eng. Chem. Res.* **1995**, *34*, 2142–2147.
(30) Celestian, A. J.; Clearfield, A. *J. Mater. Chem.* **2007**, *17*, 4839–4842.
(31) Celestian, A. J.; Kubicki, J. D.; Hanson, J.; Clearfield, A.; Parise, J. B. *J. Am. Chem. Soc.* **2008**, *130*, 11689–11694.
(32) Celestian, A. J.; Parise, J. B.; Smith, R. I.; Toby, B. H.; Clearfield, A. *Inorg. Chem.* **2007**, *46*, 1081–1089.
(33) Sava, D. F.; Kravtsov, V. C.; Nouar, F.; Wojtas, L.; Eubank, J. F.; Eddaoudi, M. *J. Am. Chem. Soc.* **2008**, *130*, 3768–3770.
(34) Fang, Q.; Zhu, G.; Xue, M.; Wang, Z.; Sun, J.; Qiu, S. *Cryst. Growth Des.* **2008**, *8*, 319–329.
(35) Yan Liu, G. L.; Xing, Li; Yong, Cui *Angew. Chem., Int. Ed.* **2007**, *46*, 6301–6304.
(36) Liu, Y.; Kravtsov, V. C.; Eddaoudi, M. *Angew. Chem., Int. Ed.* **2008**, *47*, 8446–8449.
(37) Nouar, F.; Eckert, J.; Eubank, J. F.; Forster, P.; Eddaoudi, M. *J. Am. Chem. Soc.* **2009**, *131*, 2864–2870.
(38) Plabst, M.; Bein, T. *Inorg. Chem.* **2009**, *48*, 4331–4341.

Table 1. Lattice parameters of **NaLa(H$_4$L)$_{dehyd}$**, **LiLa(H$_4$L)**•4H$_2$O, **NaLa(H$_4$L)**•4H$_2$O, **KLa(H$_4$L)**•(2+x)H$_2$O, and **RbLa(H$_4$L)**•2H$_2$O

	NaLa(H$_4$L)$_{dehyd}$	LiLa(H$_4$L)	NaLa(H$_4$L)	KLa(H$_4$L)	RbLa(H$_4$L)
cryst. system	monoclinic	monoclinic	monoclinic	monoclinic	monoclinic
space group	$P2_1/n$	$P2_1/n$	$P2_1/n$	$P2_1/n$	$P2_1/n$
a (Å)	7.165(2)	8.760(2)	8.975	9.162(5)	9.291(3)
b (Å)	22.758(5)	22.09(1)	21.691	21.88(1)	21.717(7)
c (Å)	10.147(2)	10.146(3)	10.186	10.284(9)	10.324(7)
β (deg)	100.98(2)	104.40(2)	105.56	106.49(6)	109.03(4)
V (Å^3)	1624(4)	1902(1)	1910.2	1977(2)	1969(1)
FOM (F30)[a]	38.7	20.1	–	18.3	16.7
020 (°2θ)	7.769	8.007	8.145	8.052	8.107
110 (°2θ)	11.802	11.158	11.006	10.823	10.838

[a] FOM = figure of merit; Lattice parameters of NaLa(H$_4$L) were obtained from a single-crystal structure analysis described elsewhere.[38]

Ion-exchange. For the ion-exchange experiments, saturated aqueous solutions of LiCl, KCl, RbCl, CsCl, $MgCl_2$, $CaCl_2$, $Sr(NO_3)_2$, $BaCl_2$, $NiCl_2$, $CuCl_2$, $ZnCl_2$, $MnCl_2$, $Fe(NO_3)_3$ were prepared. Ion-exchange was performed by stirring 100 mg of **NaLa(H$_4$L)** in 10 mL of the salt solution for three days at room temperature. Then the solid was separated from the solution by filtration under reduced pressure, briefly washed with water and dried at room temperature.

Powder Diffraction Data Collection. Several different X-ray powder diffractometers were used for the characterization of these materials. A Stoe Stadi P high-throughput powder diffractometer[39] (Cu Kα radiation, Ge monochromator, transmission geometry) equipped with an image plate detector system and an *xy* sample stage was used for initial identification. A Bruker D8 Discover diffractometer (Cu Kα_1, $\theta-\theta$ reflection geometry, Vantec detector) was used to record the patterns of the alkali-ion-exchanged samples. For the measurement of **KLa(H$_4$L)**, the sample was first exposed to bidistilled water to keep the K^+ guest ions hydrated. A Stoe Stadi P diffractometer (Mo Kα radiation, Ge monochromator, transmission geometry) equipped with a high temperature cell was used for the *in situ* temperature-dependent measurements of **NaLa(H$_4$L)**. For these measurements, X-ray powder diffraction patterns were recorded from 25 to 700 °C in steps of 25 °C, at 800 °C, and after cooling down to 100 °C. The sample was heated at each target temperature for 20 min before the diffraction measurement was started. Finally, a Stoe Stadi P diffractometer (Cu Kα_1, transmission mode, linear position-sensitive detector) was used to record the pattern of **NaLa(H$_4$L)$_{dehyd}$** (sealed in a 0.3 mm glass capillary) for structure analysis.

Further Characterization Methods. All of these characterization methods were applied on samples dried in air for two weeks to ensure that the samples had reached their equilibrium in the hydration/dehydration process. Morphology and stoichiometry were studied with a Joel JSM 6500 F scanning electron microscope equipped with an EDX detector. Each sample was applied to an adhesive carbon film on the sample holder and coated with carbon using a BAL-TEC MED 020 Coating System. Thermogravimetric analyses (TGA) were performed on a Netzsch STA 449 C TG/DSC (heating rate of 10 K/min in a ~25 mL/ min stream of synthetic air). The chemical compositions of the alkali-ion-exchanged samples were determined by inductively coupled plasma optical emission spectroscopy (ICP-OES, VARIAN VISTA) and compared with the EDX analysis results.

Unit Cell Determination. The powder diffraction patterns of **NaLa(H$_4$L)$_{dehyd}$** and the alkali ion-exchanged samples **LiLa(H$_4$L)**, humidified **KLa(H$_4$L)**, and **RbLa(H$_4$L)** were indexed using the Visser algorithm implemented in the program WinXPOW.[40] The results of a subsequent refinement of the lattice parameters in $P2_1/n$ are given in Table 1. Lattice parameters of the as-synthesized **NaLa(H$_4$L)** were obtained from a single-crystal structure analysis described elsewhere.[38]

Table 2. Chemical Composition of Ion-Exchanged Samples As Determined by ICP-OES

Sample	Na/P	M/P	La/P	P
NaLa(H$_4$L)	1.0	–	1.1	4.0
$Na_{(1-x)}Li_xLa(H_4L)$	0.1	1.4	1.1	4.0
$Na_{(1-x)}K_xLa(H_4L)$	0.1	1.2	1.1	4.0
$Na_{(1-x)}Rb_xLa(H_4L)$	0.1	1.1	1.1	4.0
$Na_{(1-x)}Cs_xLa(H_4L)$	0.9	[a]	1.1	4.0

[a] Cesium could not be detected in ICP-OES analysis. EDX analysis confirms a very low Cs content of the sample ($Na_{0.9}Cs_{0.2}La_{1.1}(H_4L)$).

Results and Discussion

Ion Exchange. The Na^+ ions in the channels of **NaLa(H$_4$L)** are exchangeable. Ion exchange reactions were performed with monovalent ions (Li^+, K^+, Rb^+ and Cs^+), divalent ions (Mg^{2+}, Ca^{2+}, Sr^{2+}, Ba^{2+}, Ni^{2+}, Cu^{2+}, Zn^{2+}, Mn^{2+}) and the trivalent Fe^{3+} ion. The saturated solutions of $FeCl_3$ (pH = 0) and $ZnCl_2$ (pH = 2) proved to be too acidic, and the **NaLa(H$_4$L)** framework decomposed. In all other cases, the XRD patterns and SEM images showed that the structure and morphology remained intact during the treatment (Figure S4, Supporting Information). Strikingly, EDX analysis and ICP-OES revealed that ion exchange was selective toward monovalent ions (Table 2). Na^+ (r = 1.02 Å)[41] could be replaced almost completely by Li^+ (r = 0.76 Å),[41] K^+ (r = 1.38 Å),[41] and Rb^+ (r = 1.52 Å).[41] However, the Cs^+ ion, with an ionic radius of 1.67 Å,[41] appears to be too large. Only a slight decrease in the sodium content was observed in that sample.

In contrast, samples that were treated with solutions of divalent ions showed no decrease in the sodium content (Supporting Information, Table S5), although they are smaller in size than most of the monovalent ions. The small amounts of divalent ions detected in the samples can be attributed to adsorption on the surface of the crystals. The discrimination for monovalent ions is remarkable, as absolute selectivity is rare in inorganic open-framework ion-exchange materials, and is usually related to size rather than charge. To the best of our knowledge, no open framework that accepts monovalent ions, but totally excludes more highly charged ions has ever been reported. A better understanding of this highly unusual selectivity could be gained by studying the relationships between the guest ions, the water molecules and the framework of **NaLa(H$_4$L)**.

Hydration and Dehydration. The as-synthesized form of **NaLa(H$_4$L)**, with the chemical composition NaLa[$(PO_3H)_2$-CH−C_6H_4−CH$(PO_3H)_2$]•4H$_2$O, has four water molecules per unit cell. Heating the compound to 100 °C leads to an endothermal mass loss of 11% (Figure 2). This corresponds exactly to the nominal mass fraction of water in the crystal. After the water loss, a plateau that is stable up to 375 °C is reached in the TGA diagram, indicating the presence of a stable dehydrated phase **NaLa(H$_4$L)$_{dehyd}$**.

Temperature-dependent XRD measurements support this conclusion (Figure 3). The X-ray diffraction pattern of **NaLa(H$_4$L)** remains unchanged up to 100 °C, and then a phase change occurs. The second phase is stable up to 375 °C, and between 400 and 500 °C, an amorphous product is formed. At 525 °C, oxidation leads to the formation of dense $NaLa(PO_3)_4$. While the formation of the dense high-temperature phase is an

(39) Stock, N.; Bein, T. *Angew. Chem, Int. Ed.* **2004**, *43*, 749–752.
(40) *WinXPOW 2.1.1*; Stoe & Cie GmbH: Darmstadt, Germany 2004.
(41) Shannon, R. *Acta Crystallogr., Sect. A* **1976**, *32*, 751–767.

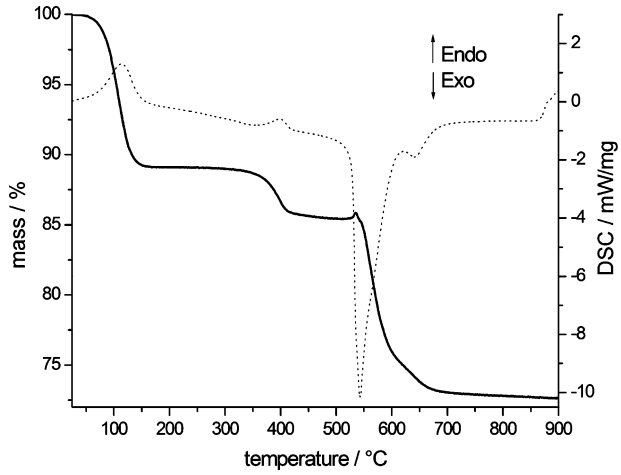

Figure 2. Thermogravimetric analysis and DSC of **NaLa(H$_4$L).**

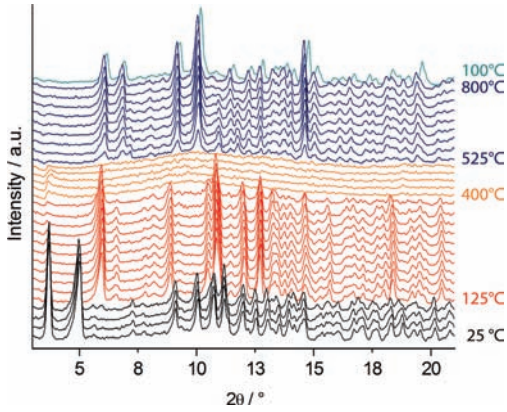

Figure 3. X-ray powder diffraction patterns (MoKα, in air) of **NaLa(H$_4$L)** (black) as a function of temperature. It transforms first to **NaLa(H$_4$L)$_{dehyd.}$** (red), and then, via an amorphous intermediate (yellow), to dense NaLa(PO$_3$)$_4$ (blue). The first low-angle peak for **NaLa(H$_4$L)$_{dehyd}$** was not recorded, because it lies outside the 2θ window of the furnace.

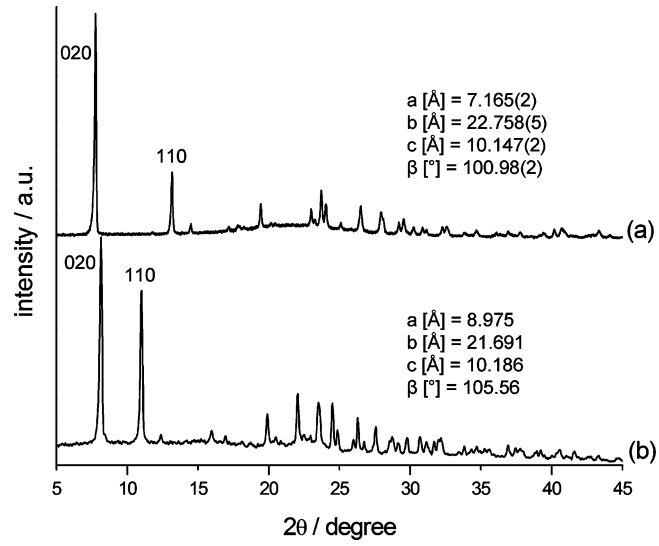

Figure 4. X-ray powder diffraction patterns (Cu Kα_1) and the corresponding lattice parameters of (a) **NaLa(H$_4$L)$_{dehyd}$** under vacuum, and (b) **NaLa(H$_4$L)** in air.

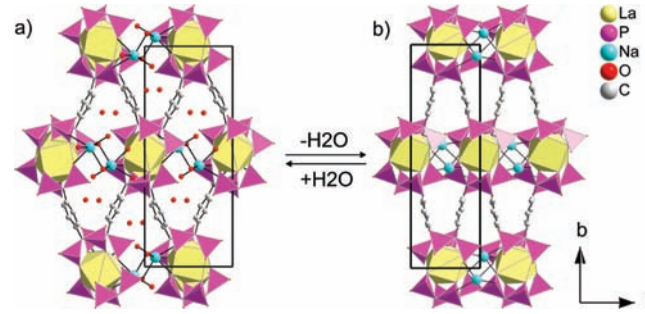

Figure 5. Contraction and expansion of the channels in **NaLa(H$_4$L)** during the dehydration/hydration process: [001] projection of the crystal structure of (a) **NaLa(H$_4$L)**, and (b) **NaLa(H$_4$L)$_{dehyd}$**. Hydrogen atoms have been omitted for clarity.

irreversible process, the first phase transformation is reversible. The water is removed upon heating, and **NaLa(H$_4$L)$_{dehyd}$** is formed. Cooling **NaLa(H$_4$L)$_{dehyd}$** to room temperature in the presence of water (e.g., from moisture in the air) allows it to transform back to the original hydrated form **NaLa(H$_4$L)**. If no water is present in the atmosphere, **NaLa(H$_4$L)$_{dehyd}$** is stable at room temperature.

During this transformation, the lanthanum phosphonate framework of **NaLa(H$_4$L)** remains intact, but the unit cell changes significantly. A comparison of the powder patterns of **NaLa(H$_4$L)** and **NaLa(H$_4$L)$_{dehyd}$** shows that they are similar, but that the peaks are shifted substantially in 2θ (Figure 4). The most obvious changes are the shifts of the 020 reflection to a lower 2θ value (corresponding to a stretching of the *b*-axis from 21.691 to 22.758(5) Å), and of the 110 reflection to a much higher value (corresponding to a shortening of the *a*-axis from 8.975 to 7.165(2) Å). Refinement of the lattice parameters shows that the cell volume decreases by 15% upon dehydration, from 1910 to 1624 Å^3 (Table 1). The change in the unit cell volume reflects the shrinking of the channels upon dehydration that was found in the structure refinement.

A complete model of the structure of **NaLa(H$_4$L)$_{dehyd}$** could be derived from the Rietveld refinement (Figure 5). The fractional coordinates of the La, Na, P, C and phosphonate O atoms from the single-crystal structure analysis of **NaLa(H$_4$L)** were used to generate a structural model for **NaLa(H$_4$L)$_{dehyd}$**. The two free water molecules and the two water molecules coordinated to Na were not included, so it was assumed that the Na$^+$ ions would adopt a tetrahedral geometry. Restraints were imposed on the bond distances (C−C, C−P, P−O, La−O, Na−O) and angles (tetrahedral P, trigonal planar C, tetrahedral Na), and the geometry was optimized for the smaller unit cell. The powder diffraction pattern of this idealized structure appeared to match the measured one quite well, so it was used as a starting point for Rietveld refinement using the XRS-82 suite of programs.[42] It soon became apparent that the angle restraints on the Na position were hindering the refinement, so they were removed. This resulted in a significant improvement in the *R*-values and a new coordination environment for the Na$^+$ ions. Further refinement of the atomic positions and displacement factors converged with $R_F = 0.056$ and $R_{wp} = 0.086$ ($R_{exp} = 0.075$). Positions for the H atoms bonded to C atoms were calculated and added to the final model, but were not refined. The positions of the H atoms of the terminal P−OH groups could not be calculated, so the occupancy parameters for these O atoms were increased to 1.125 to approximate the extra electron of the H atom. All displacement factors were

(42) Baerlocher, C.; Hepp, A. *XRS-82*; Institut für Kristallographie: Zürich, Switzerland, 1982.

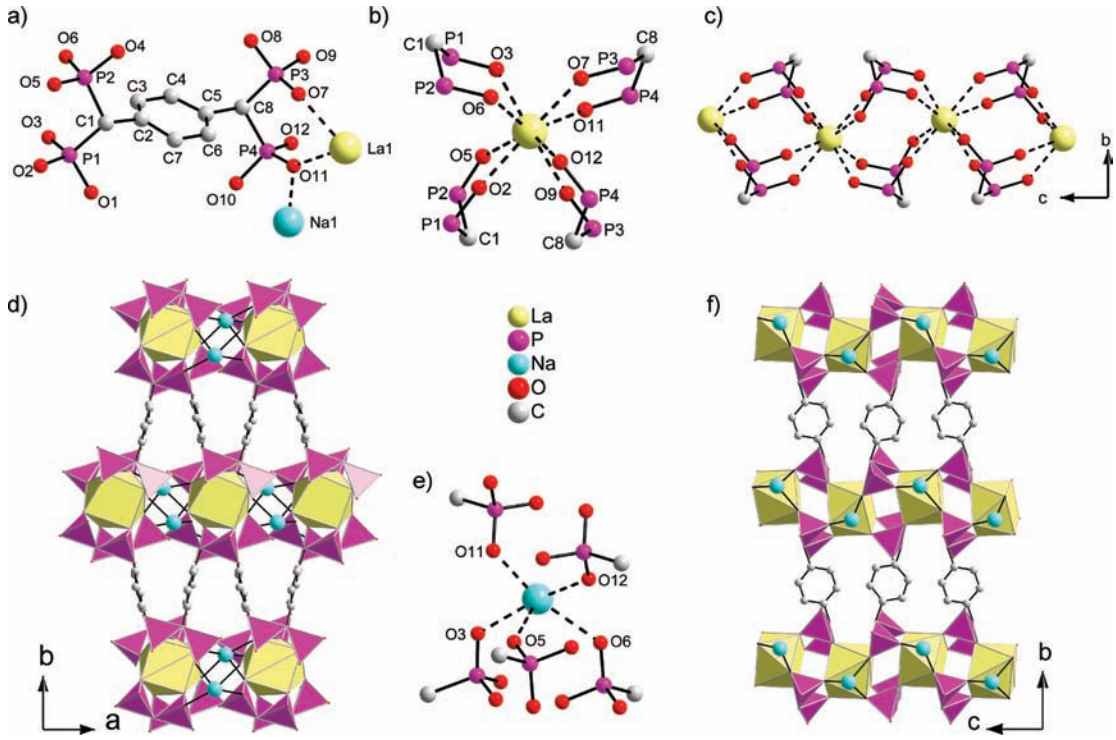

Figure 6. Structure of NaLa[$(PO_3H)_2CH-C_6H_4-CH(PO_3H)_2$], **NaLa(H$_4$L)$_{dehyd}$**. (Hydrogen atoms are omitted for clarity.) (a) Asymmetric unit, (b) coordination of La^{3+}, (c) phosphonate-bridged chain of lanthanum running along *c*, (d) projection down [001] showing the rhombus formed by the La^{3+} ions and the bisphosphonate linkers, (e) coordination of Na^+, (f) projection of down [100] showing the decoration of the −La−O−P−O−La− chains with sodium ions.

refined isotropically, and those for similar atoms were constrained to be equal to keep the number of parameters to a minimum. Neutral scattering factors were used for all atoms. The final atomic parameters for this model are provided as a CIF file in the Supporting Information. Details of the refinement are given in Table S1 (Supporting Information), and selected bond distances in Table S2 (Supporting Information). The fit of the calculated powder diffraction pattern to the measured data is shown in Figure S1 (Supporting Information).

The asymmetric unit of **NaLa(H$_4$L)$_{dehyd}$** contains 26 non-hydrogen atoms (Figure 6a). The crystal structure is composed of $[(PO_3H)_2CH-C_6H_4-CH(PO_3H)_2]^{4-}$, La^{3+}, and Na^+ ions. From the P−O distances it is apparent that all four phosphonic acid groups are singly deprotonated (Table S2a, Supporting Information). As in **NaLa(H$_4$L)**,[38] the La^{3+} ions are each coordinated to 8 phosphonate oxygens of four $(H_4L)^{4-}$ ligands. The La−O distances range from 2.47(2) to 2.70(2) Å (Table S2b, Supporting Information). These are slightly longer than those in **NaLa(H$_4$L)**, but are still comparable to those reported for $LaPO_4$.[43] As in **NaLa(H$_4$L)**, lanthanum is coordinated only to bisphosphonate oxygen atoms (Figure 6b). Each phosphonate group bridges between neighboring lanthanum ions in such a way that an −La−O−P−O−La− chain is built along *c* (Figure 6c). The coordinating oxygen atoms around lanthanum form a distorted square antiprism with the top square decorated with the P1 and P2 and the bottom square with the P3 and P4 phosphonate groups. The structure is completed with the benzene spacer connecting the bisphosphonate groups (Figure 6d and 6f) to form a three-dimensional open framework with the −La−O−P−O−La− chains located at the corners of a rhombus (Figure 6d). The rhombic channels along *c* that are observed in **NaLa(H$_4$L)** are contracted in **NaLa(H$_4$L)$_{dehyd}$**. The main openings in this contracted form are small apertures between terminal P−OH groups (O···O: 3.60 Å) and between the benzene linkers (C···C: 4.52 Å) that can be observed along the [101] direction (Figure S3-1). Sodium ions reside as guests in the pores, where each is coordinated to five phosphonate oxygens in a square pyramidal arrangement (Figure 6e) with Na−O distances ranging from 2.30(2) Å to 2.73(2) Å (Table S2c, Supporting Information).[44] The Na^+ ion coordinates to three phosphonate oxygens bridging to one La^{3+} ion (O3, O5 and O11) and to two others (O12 and O6) bridging to a second La^{3+} ion in an adjacent −La−O−P−O−La− chain. Thus, the Na^+ ions are located opposite triangular faces of the lanthanum polyhedron on both sides of the −La−O−P−O−La− chain (Figure 6f).

A comparison of the structure of **NaLa(H$_4$L)$_{dehyd}$** with that of **NaLa(H$_4$L)** gives detailed insights into the mechanism of the channel shrinkage and the role of the guest ion in this process. Of the four water molecules in the channels of **NaLa(H$_4$L)**, two are free and two are coordinated to sodium (Na−O13, 2.402(2) Å and Na−O16, 2.215(2) Å). In this hydrated expanded form, each Na^+ ion is also coordinated to three phosphonate O atoms (O3, O5, and O11 with Na−O distances of 2.531(2), 2.353(2), and 2.296(2) Å), which bridge to a single La^{3+} ion. Sodium ions decorate alternating sides of the lanthanide phosphonate chains running along the [001] direction (Figures 5a and 7a). The octahedral coordination sphere of Na^+ is completed with a rather weak bond (Na−O10 = 2.665(2) Å) to a protonated P−OH group of a neighboring lanthanum phosphonate chain. Upon dehydration, all of the

(43) Jaulmes, S. *Bull. Soc. Fr. Min. Crist.* **1972**, *95*, 42–46.

(44) Averbuch-Pouchot, M. T.; Durif, A. *J. Solid State Chem.* **1983**, *46*, 193–196.

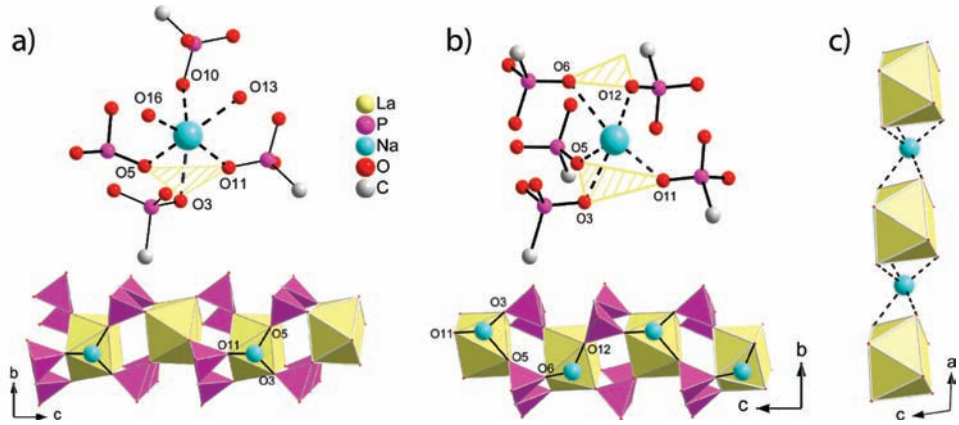

Figure 7. Coordination sphere of sodium and its location in the metal phosphonate chain in (a) **NaLa(H$_4$L)**, and (b) **NaLa(H$_4$L)$_{dehyd}$**, and (c) the −La−O−Na−O−La− chain along *a* in **NaLa(H$_4$L)$_{dehyd}$**.

MLa(H$_4$L)	x H$_2$O	expanded	contracted
LiLa(H$_4$L)	4 H$_2$O	⇌	
NaLa(H$_4$L)	4 H$_2$O	⇌	
KLa(H$_4$L)	2 H$_2$O	⇌	
RbLa(H$_4$L)	2 H$_2$O	⇌	

Figure 8. Water content and equilibrium between the expanded and contracted forms of MLa(H$_4$L) in air and at room temperature.

water molecules leave the structure, and the Na^+ ion compensates for the loss of two of its ligands by forming two new bonds with phosphonate oxygens (O6 and O12) in the adjacent −La−O−P−O−La− chain (Figure 5b, Figure 7b). In this process, its sacrifices the weak Na−O10 bond, and its coordination becomes square pyramidal. As a result, an −La−O−Na−O−La− chain is generated along *a* (Figure 7c, Figure S3-2, Supporting Information). The formation of this second chain requires a shortening of *a* with a concomitant shrinking of the channels. The connectivity of the lanthanum-bisphosphonate framework remains intact, but the square antiprism coordination polyhedron of the lanthanum ions distorts by twisting the two squares with respect to one another to accommodate the effects of the dehydration (Figure S3-3, Supporting Information). This results in a decrease in the acute angle of the rhombus from 41.1° in **NaLa(H$_4$L)** to 26.4° in **NaLa(H$_4$L)$_{dehyd}$** (see Figure 5).

The −La−O−Na−O−La− chain formation can be considered to be the driving force for the channel shrinkage, and is therefore the key to understanding the flexibility of the framework. An equilibrium exists between the expanded (hydrated) and the contracted (dehydrated) form (Figure 7). In this equilibrium, the hydration energy of the guest ion competes with the lattice energy that is gained by chain formation. In the as-prepared sodium compound (in air and at room temperature), the equilibrium favors the expanded form.

The exchanged forms **LiLa(H$_4$L)** and **KLa(H$_4$L)** can also exist in both forms (Figure 8). TGA analysis shows that **LiLa(H$_4$L)** contains 4 equivalents of water (Figure S6a, Supporting Information), and like **NaLa(H$_4$L)**, is stable in the expanded form at room temperature. In **KLa(H$_4$L)** and **RbLa(H$_4$L)**, the mass losses upon heating to 100 °C correspond to only two water molecules per unit cell (Figure S6c,d, Supporting Information). The XRD pattern of **KLa(H$_4$L)** shows a slow transformation when the sample is dried in air (Figure 9), and the directions of the shifts of the 020

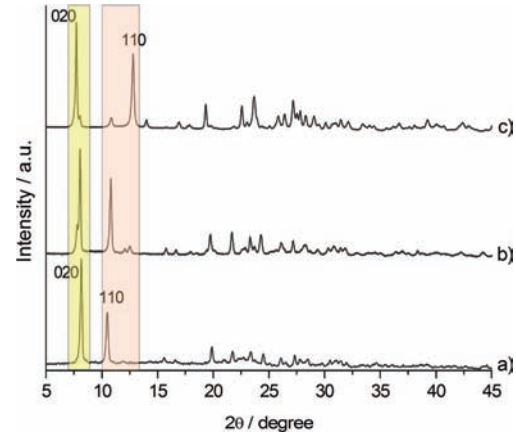

Figure 9. XRD patterns of **KLa(H$_4$L)** (a) immediately after hydration, (b) after 4 h, and (c) after one week, show that the structure slowly shifts from the expanded to the contracted form, while it is drying in air at room temperature. Yellow region, 020 shift; Red region, 110 shift.

and 110 reflections correspond to those observed for **NaLa(H$_4$L)** upon dehydration. It can be concluded that in the case of **KLa(H$_4$L)**, the equilibrium favors the contracted form, but the energy barrier between the two forms is very low. Hydrating the sample with a drop of water causes an immediate shift back to the expanded form.

Under the same conditions, only one XRD pattern is observed for **RbLa(H$_4$L)** (Figure S4b, Supporting Information). The lower water content and the positions of the reflections in the XRD pattern are indicative of a contracted form. All attempts to obtain an expanded form by hydrating the sample were unsuccessful. This can be explained by the fact that Rb^+ has a lower enthalpy of hydration than do the smaller alkali metal ions and that the larger Rb^+ ion is well-accommodated in a more contracted coordination environment.

The ionic guests play a crucial role in the chain-forming/breaking mechanism that determines the flexibility of the framework. Different monovalent ions with different ionic radii and enthalpies of hydration influence the equilibrium between the expanded and the contracted forms differently. Although they are exchangeable, the monovalent ions are located at a specific site in the structure, where they contribute significantly to its stabilization.

The strong interaction between the guest and the framework becomes even more apparent when the positions of the reflections in the diffraction patterns of the exchanged samples

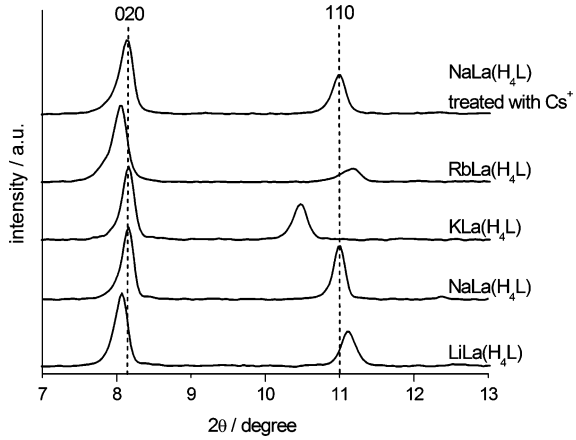

Figure 10. Shifts of the 020 and the 110 reflections in the powder patterns of **LiLa(H$_4$L)**, **NaLa(H$_4$L)**, **KLa(H$_4$L)**, **RbLa(H$_4$L)**, and of **NaLa(H$_4$L)** after the treatment with Cs^+.

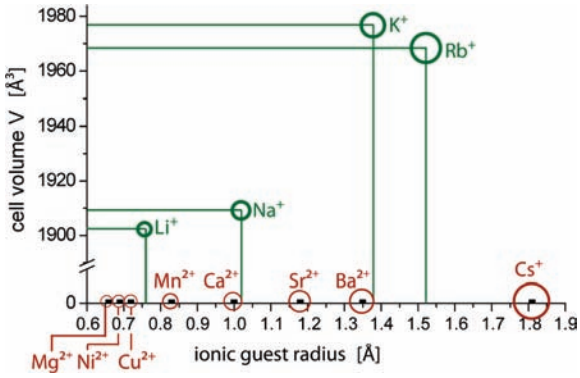

Figure 11. Radii of the ions, which are uptaken (green) or not uptaken (red) by the framework of **MLa(H$_4$L)** and correlation with the respective cell volume in its highest observed hydrated state: **LiLa(H$_4$L)**•4H$_2$O dried in air, **NaLa(H$_4$L)**•4H$_2$O, dried in air; **KLa(H$_4$L)**•(2+x)H$_2$O, humidified; **RbLa(H$_4$L)**•2H$_2$O humidified or dried in air.

are compared. It can be seen that the framework not only changes by forming a −La−O−M(I)−O−La− chain, but that it also adapts to the size of the incorporated ion (Figure 10). In the pattern of the Li^+ exchanged samples, the 110 reflection is shifted to a 2θ value higher than that of **NaLa(H$_4$L)**. This corresponds to a contraction of the channels and is therefore in good agreement with the fact that lithium is smaller than sodium. The pattern of the K^+-exchanged sample shows a shift of the 110 reflection in the opposite direction, as would be expected for the expansion needed to accommodate the larger cation. As **RbLa(H$_4$L)** is present in a contracted form, the shifts are reversed. The 2θ value of the 100 reflection is larger than that for **KLa(H$_4$L)**, indicating a decrease in the channel size. As Cs^+ does not enter the channels, the sample treated with cesium does not show any change in the powder diffraction pattern from that of the Na-form. The adaptation of the framework to the size of the guest ion is reflected in the unit cell volumes (Figure 11). The changes are smaller than that observed for **NaLa(H$_4$L)** upon dehydration, but still noticeable, and range from 1902 Å^3 for **LiLa(H$_4$L)** to 1977 Å^3 for **KLa(H$_4$L).** Comparison of the five materials discussed in this study shows that a change in the unit cell volume of 22% is observed in going from **NaLa(H$_4$L)$_{dehyd}$** to **KLa(H$_4$L)**.

From these observations it can be deduced that the ionic guests are more than charge equalizers and space fillers. The strong response of the framework to the ionic guest explains the enhanced selectivity of **NaLa(H$_4$L)** for monovalent cations. To maintain charge balance, divalent cations could only occupy every second guest site, and this might reduce the stability of the framework and make the incorporation of divalent cations difficult. **NaLa(H$_4$L)** has been shown to be an ion exchanger, where the effect of framework adaptation on ion-exchange selectivity, which plays only a minor role in zeolites, is fundamental.

Conclusions

The sodium lanthanide tetrakisphosphonate NaLa[$(PO_3H)_2$-CH−C_6H_4−$CH(PO_3H)_2$]•4H$_2$O, **NaLa(H$_4$L)** features a flexible open-framework anionic host with an extraordinary charge selectivity for its guest cations. In aqueous media, the Na^+ ions hosted in the channels of the structure can be exchanged with other monovalent ions with ionic radii ranging from 0.76 Å (Li^+) to 1.52 Å (Rb^+), while divalent ions in the same size range are rejected. The water molecules in the channels can be removed by heating, and this causes a shrinking of the channels and a decrease in the cell volume of 15%. Upon dehydration, the Na^+ ions compensate for the loss of coordinated water by forming new bonds with phosphonate oxygens, and in the process generate an −La−O−Na−O−La− chain perpendicular to the lanthanum phosphonate chain of the original coordination network. The formation of this second chain stabilizes the framework and can be considered to be the driving force for the structural transformation. This dehydration process is fully reversible. The ion-exchanged compounds **LiLa(H$_4$L)** and **KLa(H$_4$L)** can exist in both the expanded and the contracted forms, whereas **RbLa(H$_4$L)** is found only in a contracted form. The ionic radius and the enthalpy of hydration of the guest cation were seen to influence the equilibrium between the two forms. The framework adapts to the water content or the guest cation, and a volume change of 22% was observed in going from the dehydrated contracted Na^+ form to the expanded hydrated K^+ form. The key role played by the ionic guest in the chain-forming mechanism and the adaptation of the framework to the size of the cation both show the relevance of the exchangeable cations to framework stabilization and charge balance. The monovalent guest cations are located at specific sites in the structure, where they can satisfy their coordination requirements. Divalent ions could occupy only half of these sites, and this might explain the unusual selectivity of this material for monovalent cations. The type of framework flexibility observed for the lanthanide tetrakisphosphonate **NaLa(H$_4$L)** suggests new opportunities for the design of chemically selective sensors and selective ion-exchange materials from MOF materials with flexible anionic frameworks.

Acknowledgment. Funding from the DFG is gratefully acknowledged. We thank T. Miller from the Department of Chemistry and Biochemistry of the Ludwig-Maximilians-University of Munich for the temperature-dependent XRD experiments. The authors thank S. Schmidt from the Department of Chemistry and Biochemistry of the LMU for scanning electron microscopy and EDX analysis.

Supporting Information Available: The Rietveld plot, crystallographic data for **NaLa(H$_4$L)$_{dehyd}$**, selected bond distances in the structure model for **NaLa(H$_4$L)$_{dehyd}$**, additional illustrations comparing **NaLa(H$_4$L)** with **NaLa(H$_4$L)$_{dehyd}$**, XRDs of ion-exchanged samples, results of EDX analysis, TGA and DSC curves for **RbLa(H$_4$L)**, and crystallographic data for **NaLa(H$_4$L)$_{dehyd}$** in CIF format. This material is available free of charge via the Internet at http://pubs.acs.org.

JA904636Y